sciendo
ARTIFICIAL SATELLITES, Vol. 58, No. 4 – 2023
DOI: 10.2478/arsa-2023-0013

ESMGFZ EAM PRODUCTS FOR EOP PREDICTION: TOWARD THE QUANTIFICATION OF TIME VARIABLE EAM FORECAST ERRORS

Robert DILL, Henryk DOBSLAW, Maik THOMAS

Helmholtz Centre Potsdam, GFZ German Research Centre for Geosciences, Potsdam, Germany

e-mail: dill@gfz-potsdam.de

ABSTRACT. Since more than 10 years, the Earth system modeling group at GFZ (ESMGFZ) provides effective angular momentum (EAM) functions for Earth orientation parameter assessment on a routinely daily basis. In addition to EAM of the individual Earth's subsystems atmosphere, ocean, and hydrology, the global mass balance is calculated as barystatic sea level variation by solving explicitly the sea-level equation. ESMGFZ provides also 6-day forecasts for all of these EAM products. EAM forecasts are naturally degraded by forecast errors that typically grow with increasing forecast length, but they also show recurring patterns with occasionally higher errors at very short forecast horizons. To characterize such errors which are not randomly distributed in time, we divided the errors into a systematic and a stochastic contribution. In an earlier study, we were able to detect and remove the large systematic fraction occurring in the atmospheric angular momentum (AAM) wind term forecast errors with a cascading forward neural network model, thereby reducing the total forecast error by about 50%. In contrast, we were not able to remove the random error component assed in this study. Nevertheless, we show that machine learning methods are able to predict quasi-daily variations in time variable EAM forecasts error levels. We plan to provide these forecast error estimates along with the deterministic EAM forecast products for subsequent use in, for example, EOP Kalman filter prediction schemes.

Keywords: effective angular momentum function, machine learning, forecast error, level of uncertainty

1. INTRODUCTION

Time variations in the orientation of the solid Earth are largely governed by the exchange of angular momentum with the surface geophysical fluids of atmosphere, oceans, and the land surface. Modeled fields of atmospheric winds, atmospheric surface pressure, ocean currents, ocean bottom pressure, and terrestrial water storage allow to calculate effective angular momentum (EAM) functions that provide highly reliable information about changes in the orientation of the Earth's rotation axis and rotational speed. The influence of atmospheric surface pressure and winds on variations in Earth rotation has been already demonstrated by Barnes et al. (1983), who introduced EAM for the first time. EAM summarizes the angular momentum changes from mass redistributions in any of the Earth subsystem's atmosphere, ocean, and land hydrology to the overall effect on the orientation of the solid Earth with respect

©The Author(s). This is an open-access article distributed under the terms of the Creative Commons Attribution License (CC BY 4.0, https://creativecommons.org/licenses/by/4.0/), which permits use, distribution, and reproduction in any medium, provided that the Article is properly cited.

to the celestial reference frame (Brzezinski, 1992). In addition to the matter term related to the time variable mass distribution, EAM also contains the motion term derived from relative angular momentum changes such as vertically integrated zonal and meridional atmospheric winds. EAM functions intrinsically consider a partly decoupled rotation of the Earth's core, the effect of elastic Earth surface deformations under atmospheric pressure, and rotational deformations.

EAM can be also calculated from atmospheric, oceanic, and hydrological model forecasts. Comparing such EAM forecasts with subsequently calculated EAM analysis shows significant high prediction skills for about 5 days into the future. For longer prediction horizons, EAM forecast prediction skills decrease rapidly for atmospheric angular momentum (AAM), but for oceanic angular momentum (OAM) and hydrological angular momentum (HAM), there is still some useful information on longer prediction horizons, indicating that low-frequency oceanic and hydrospheric processes can substantially extend the window of predictability (Dill et al., 2013). In recent years, more and more studies included such EAM forecasts into Earth's orientation prediction approaches. Especially, the short-term predictions of variations in the Earth's spin rate universal time–coordinated universal time (UT1–UTC) are dominated by the third component of AAM forecasts. UT1 prediction errors were reduced by 20% at a forecast horizon of 5 days (Bell et al., 1991). However, it also showed that including the AAM forecasts sometimes degraded the UT1 prediction skill due to systematic differences between AAM forecasts and the UT1 series (Freedman et al., 1994). Smoothing of the AAM data to reduce the sub-daily variability helped to mitigate those effects, albeit on the expense of losing temporal detail. Using neural network prediction approaches, the system can be trained to ignore AAM forecast errors while extracting only the reliable information (Modiri et al., 2020, Kiani et al., 2022a).

Not only UT1 and length of day (LOD) predictions, but also the polar motion predictions could be improved by AAM forecasts. Moreover, OAM and HAM forecast data have become very valuable for better Earth orientation parameter (EOP) prediction (Dill & Dobslaw, 2010). Although EAM forecasts have typically a forecast horizon of only several days, 90-day EOP predictions benefit as well from including EAM forecast data in the EOP prediction approach (Dill et al., 2018).

Nowadays, EAM forecasts are frequently used in many advanced EOP prediction methods (see e.g., the second EOP prediction comparison campaign [EOPPCC], http://eoppcc.cbk.waw.pl/) including machine learning and Kalman filter techniques. All prediction techniques that show as low mean absolute errors as the official prediction of the International Earth Rotation and Reference Systems Service (IERS), called bulletin A, or even better use at least AAM forecasts or all available EAM forecasts (Kur et al., 2022). Best prediction methods also implicitly consider the EAM forecast errors by a combination of AAM forecasts with AAM analysis data (Dill et al., 2019), elimination of AAM wind term forecast errors by a cascade forward neural network (Dill et al., 2021), or generating improved EAM forecasts using machine learning (Kiani et al., 2022b; Gou et al, 2023). Although such new methods can reduce the influence of existing EAM forecast errors, a more detailed picture of the EAM forecast uncertainties is hidden in such approaches. Hence, in this contribution, we will focus more closely on the differences between EAM forecasts and subsequently available EAM analysis data as processed by the Earth system modeling group at the GFZ German Research Centre for Geosciences (ESMGFZ, http://esmdata.gfz-potsdam.de:8080/repository). Knowing EAM forecast uncertainties, they can be directly introduced into the prediction by, for example, a Kalman filter (Freedman et al., 1994) or a probabilistic machine learning method (Kiani & Soja, 2022).

2. EAM FORECAST ERRORS

Many ESMGFZ EAM forecasts are characterized by continuously growing forecast errors with increasing lead time. This particularly applies not only to all OAM, HAM, and sea-level angular momentum (SLAM) components, X_1, X_2, X_3, mass, and motion terms, but also to the X_1 and X_2 mass term forecasts of the atmosphere, which all show excellent prediction skills with Brier skill scores (von Storch and Zwiers, 1999) well above 0.8, even beyond day 6. In contrast to this good performance, AAM X_1 and X_2 motion term forecasts are characterized by substantially lower prediction skills. Brier skill scores frequently drop below zero during the first forecast days already (see Fig. 3 in Dobslaw & Dill, 2017). Quasi-periodic variations present in the forecasts that are not replicated in the later available analysis data substantially degrade EAM forecast skills, and consequently EOP prediction.

When plotting the differences between AAM forecasts and associated analyses over 7 years (Figure 1), we find that AAM forecast equatorial wind terms (AAM X_1 and X_2 motion) deviate largely from the analysis in an apparently systematic way, especially in the very first forecast epochs. In contrast, for the other AAM terms and also for all OAM and HAM terms, the differences between forecast and analysis (see Figures 2 and 3) do not contain such features, but show a rather random distribution that gradually increases with prediction length. For this study, we consider the differences between forecast and analysis as a measure of the forecast error.

In the AAM X_1 and X_2 motion term forecasts, we found artificial quasi-periodic signals with initial amplitudes larger than the increasing stochastic forecast error, with an average period of 1.071 days in X_1 and 1.098 days in X_2. From day to day, this artificial signal is excited irregularly in the numerical weather prediction system of the European Center for Medium Weather Forecast (ECMWF) with seemingly arbitrary amplitude and phase. This signal, if excited, is somewhat dampened out with increasing forecast length.

When calculating the average of all daily forecast differences, we obtain almost zero for all individual forecast epochs in the case of a stochastic error distribution. This is not the case for AAM X_1 and X_2 motion term forecasts. We denote this kind of error distribution as systematic error.

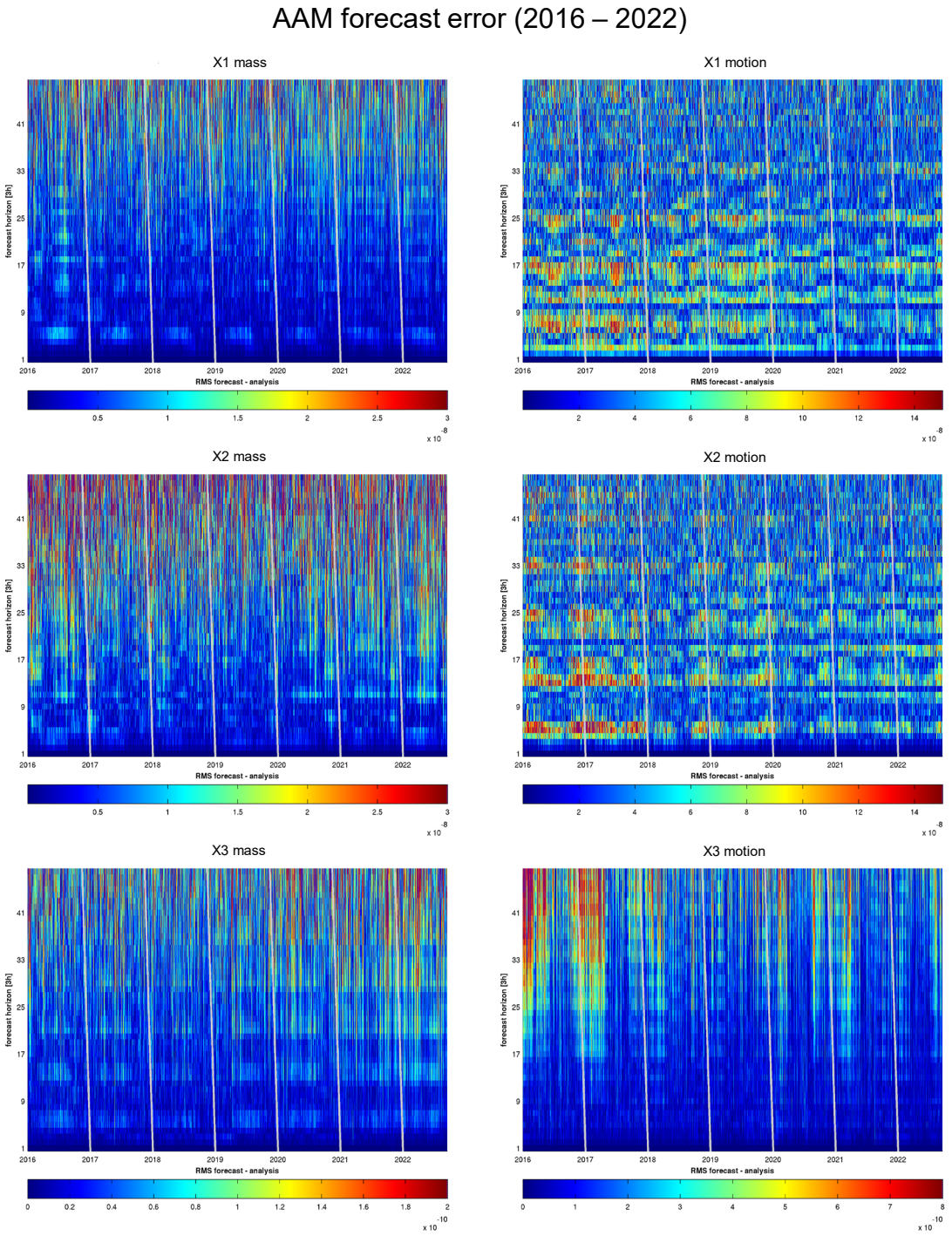


Figure 1. Root mean squared error (RMS) between AAM forecast and subsequent AAM analysis representing the forecast error for daily 6-day forecasts sampled every 3 hours from January 2016 until December 2022: AAM mass terms (left), AAM motion terms (right) for X_1 (top), X_2 (middle), and X_3 (bottom).

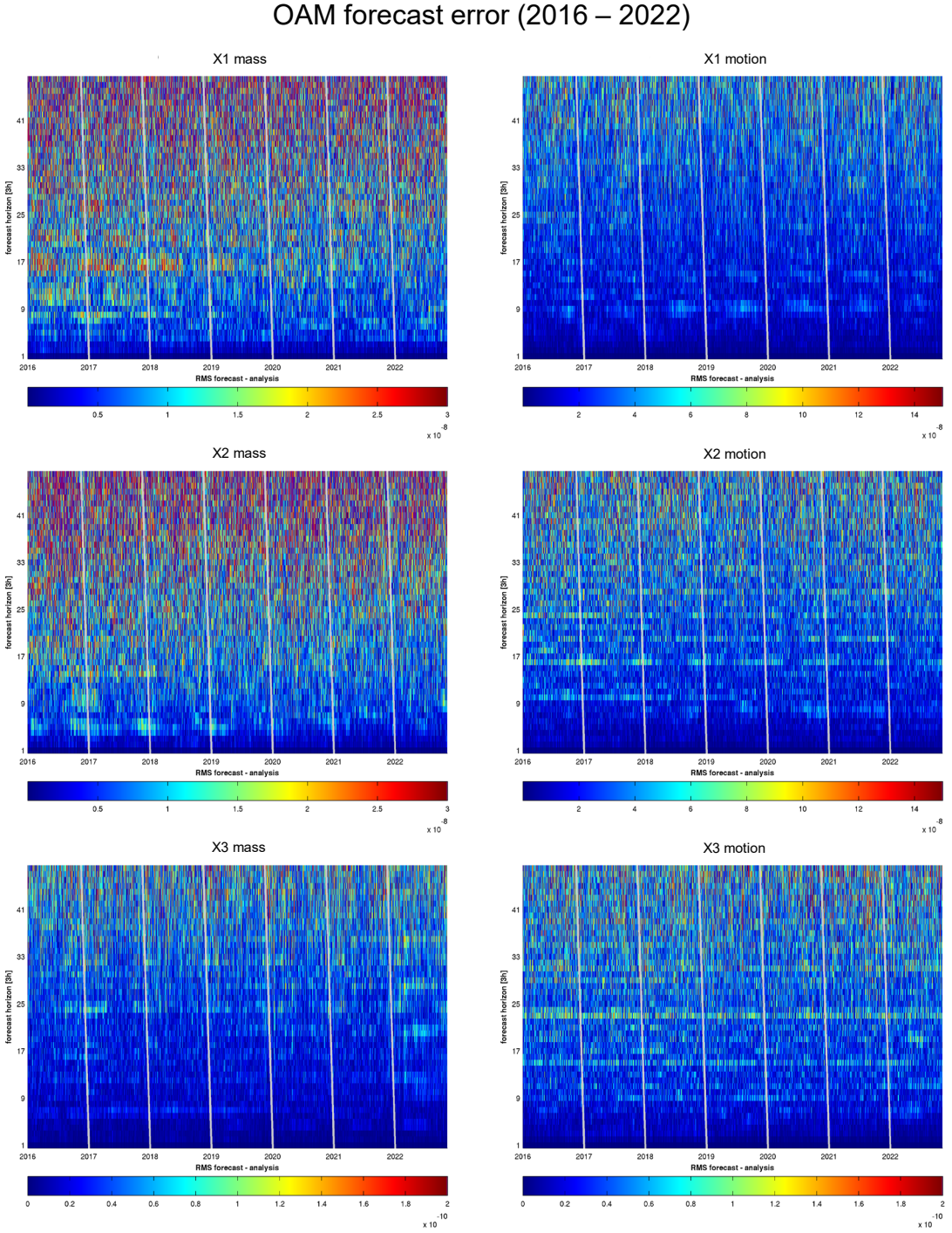


Figure 2. Root mean squared error (RMS) between OAM forecast and subsequent OAM analysis representing the forecast error for daily 6-day forecasts sampled every 3 hours from January 2016 until December 2022: OAM mass terms (left), OAM motion terms (right) for X_1 (top), X_2 (middle), and X_3 (bottom).

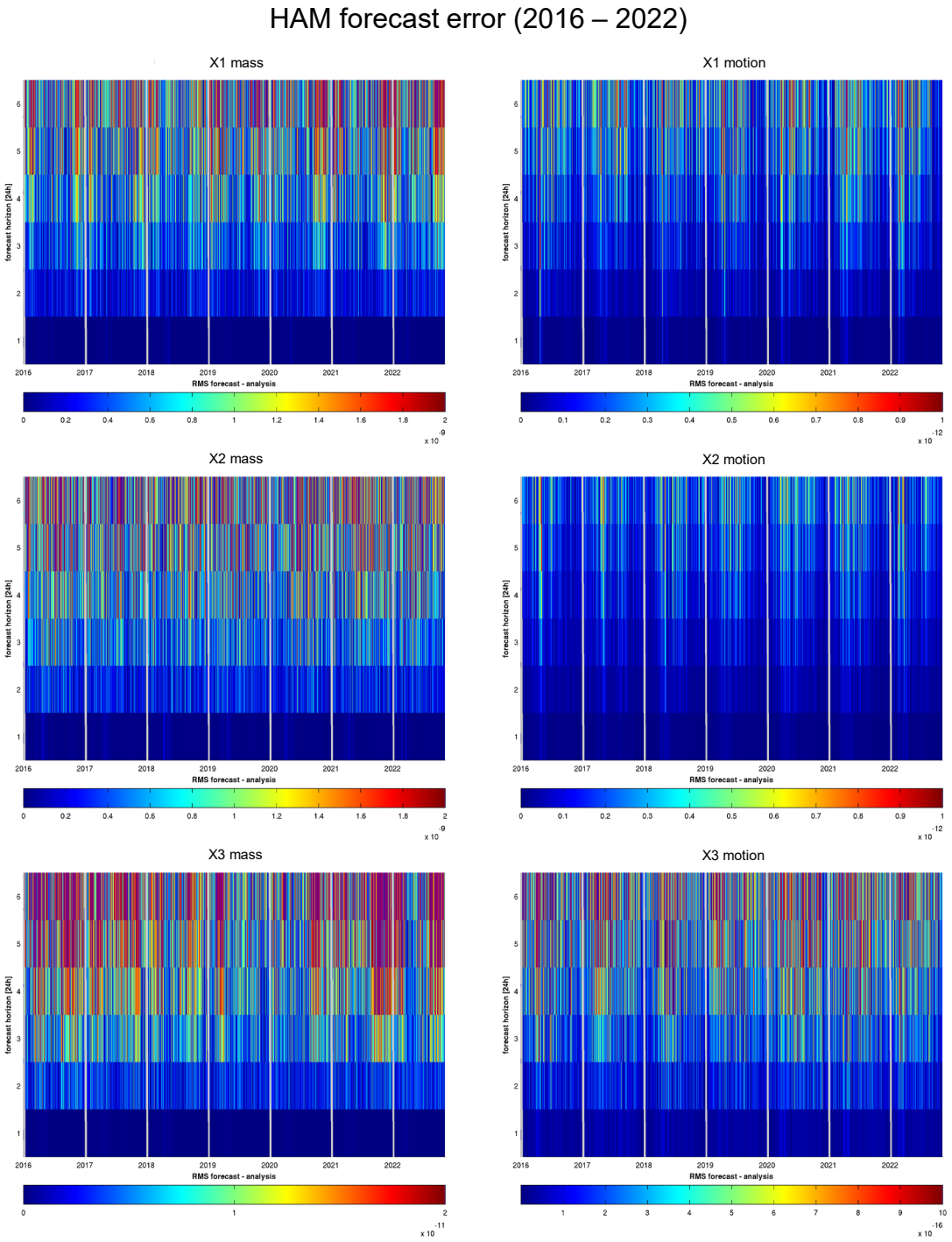


Figure 3. Root mean squared error (RMS) between HAM forecast and subsequent HAM analysis representing the forecast error for daily 6-day forecasts sampled every 24 hours from January 2016 until December 2022: HAM mass terms (left), HAM motion terms (right) for X_1 (top), X_2 (middle), and X_3 (bottom).

2.1. Assessment of systematic errors with neural networks

To detect possible systematics in these forecasts, we set up a machine learning model. We trained a cascade forward neural network with the differences between forecast and analyses separately for each EAM component. Such a trained neural network model is able to predict the artificial signals in amplitude and phase as they appear in AAM forecasts even for time steps outside the training period.

Applying such differences predicted from the neural network, AAM forecasts can be improved by removing these artificial signals (Dill et al., 2021). ESMGFZ already provides such improved AAM forecasts with corrected X_1 and X_2 motion term components as an alternative to the nominal AAM forecast product (http://esmdata.gfz-potsdam.de:8080/repository). After subtraction of the systematic error in the equatorial AAM motion term forecasts, the remaining differences between forecast and analysis follow the expected normal distribution like in any other EAM component. Please note that applying the machine learning approach to these other components of OAM and HAM does not yield any significant improvement. In other words, we are not able to reduce the stochastic part of the misfit between EAM forecast and analyses with any neural network configuration tested so far.

2.2. Influence of EAM forecast errors on EOP predictions

EOP predictions benefit a lot from the incorporation of EAM forecasts. However, improvements in the EOP predictions by including EAM data into the prediction approach are limited by the length of available EAM forecast window (here, 6 days into the future) and the EAM forecast quality. To investigate to which extent the EAM forecast quality influences the predicted EOPs, we can introduce perfect EAM forecasts (as derived from the analyses) into GFZ's EOP prediction approach.

GFZ's EOP predictions are calculated using the GFZ EAM Predictor (Dill et al., 2019). In a first step of least-squares harmonic estimation, including an autoregression model for the nonharmonic residual (LS + AR) (i.e.,), the difference between 4 years of model-based EAM functions and the geodetic angular momentum (GAM; 4 years derived from IERS 14C04) is extrapolated for the last ~30 days, where no GAM is available, up to the end of the EAM 6-day forecasts. The sum of this extrapolated GAM − EAM difference and the model-based EAM is then predicted into the future by a second step of LS + AR. EOP predictions are derived then from the 90-day EAM prediction by applying the Liouville equation with the latest available EOP coordinates from IERS rapid EOPs (finals.daily) as initial conditions.

Table 1 shows exemplarily the results of using perfect EAM forecasts, without any forecast error, for polar motion predictions up to 10 days into the future. Especially in the x-pole component, RMS could be reduced by 12.5%. If we improve the erroneous EAM forecasts by correcting the systematic errors in the AAM X_1 and X_2 motion terms, it yields at least an RMS error reduction of 5% in x-pole. Half of the total error in EAM forecasts is caused by the systematic error in the AAM motion terms.

Table 1. RMS prediction error in polar motion for forecast horizons of 5, 10, 40, and 90 days in x-pole, y-pole coordinate and 2D polar motion vector for different EAM forecast input. Black line: prediction approach using erroneous EAM forecasts; purple line: using perfect EAM forecast without any deviation from EAM analysis; yellow line: using EAM forecasts with corrected AAM X_1 and X_2 motion terms. The percentages give the improvement in RMS compared to the original RMS (black).

RMS [mas]	X pole				Y pole				X+iY pole			
2016-2020	5d	10d	40d	90d	5d	10d	40d	90d	5d	10d	40d	90d
LS+AR + EAM forecast	0.93	1.92	8.65	15.76	0.65	1.30	5.14	10.85	1.13	2.32	10.05	19.13
perfect EAM forecasts	0.88	1.68	8.56	15.80	0.66	1.28	5.10	10.74	1.10	2.11	9.97	19.10
	-5.4%	-12.5%	-1.0%	0.25%	1.5%	-1.5%	-0.8%	-1.0%	-2.7%	-9.1%	-0.8%	-0.2%
corrected AAM	0.89	1.82	8.63	15.77	0.65	1.31	5.09	10.77	1.12	2.25	10.03	19.11
	-4.3%	-5.2%	-0.2%	0.1%	0.0%	0.8%	-1.0%	-0.7%	-0.9%	-3.0%	-0.2%	-0.1%

2.3. Stochastic error – level of uncertainty prediction

The stochastic error in EAM forecasts generally increases with forecast length; however, we found very different error levels in forecasts of subsequent days. A simple linearly increasing error level would not describe sufficiently the error level of individual days. Therefore, we started to characterize those different error patterns using a feed forward neural network.

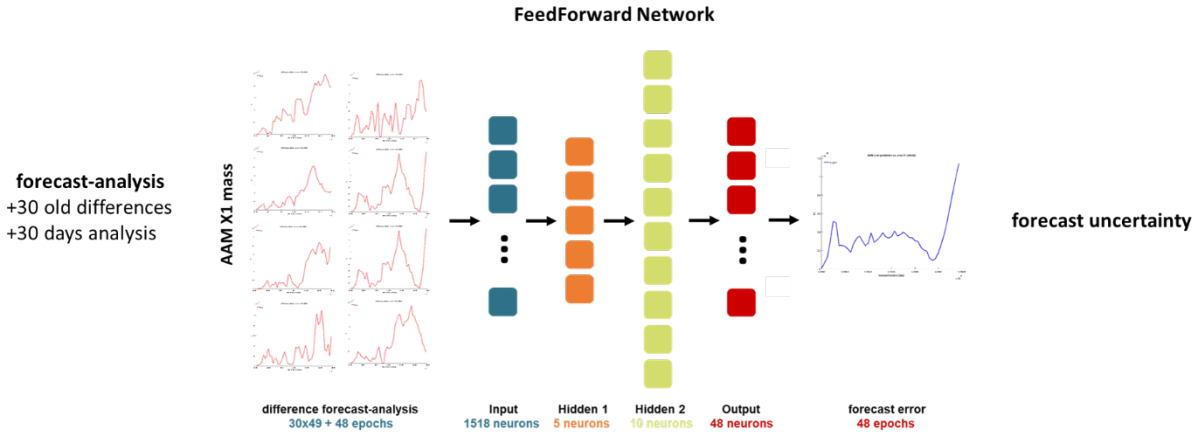


Figure 4. Neural network to predict level of uncertainty of EAM forecast. Training and input data are the absolute values of the differences between EAM forecast and EAM analysis. The target and output is the level of uncertainty of the EAM forecast. AAM and OAM forecasts are three-hourly sampled with 48 epochs for days. The input series also include one initial epoch before the forecast starts. For HAM and SLAM with only 24-hourly sampling, the input and output neurons are reduced accordingly.

Subsequently, we do not train the network with the differences between forecasts and analysis as for the systematic error, but instead use only the absolute value of those differences. We set up a feed forward network using daily 6-day forecasts and the analysis data of the last 36 days. We calculated 30 sets of absolute values from the difference between 30 individual 6-day forecasts and the related analysis data. Including the initial value before the forecast starts, they have 49 epochs with three-hourly resolution each. In addition, the network is fed with one new EAM forecast, 6 days with 48 3-hourly epochs, for which we want to estimate the unknown forecast uncertainty level (Figure 4). The first and second hidden layers consist of 5 and 10 neurons, respectively. The target is defined as the level of uncertainty, which is the absolute

value of the true forecast error. Figure 5 shows exemplarily the predicted level of uncertainty (blue) against the true forecast error (red) for eight different epochs of AAM X1 mass term forecasts. Transferable results were obtained for all the other components of EAM mass and motion terms. We are not able to predict the forecast uncertainty for all sub-daily variations in detail, but the uncertainty prediction gives a very good first guess of the variable uncertainty level for each different AAM forecast. We were able to capture also the totally different error evolution over the whole range of each 6-day forecast between consecutive days.

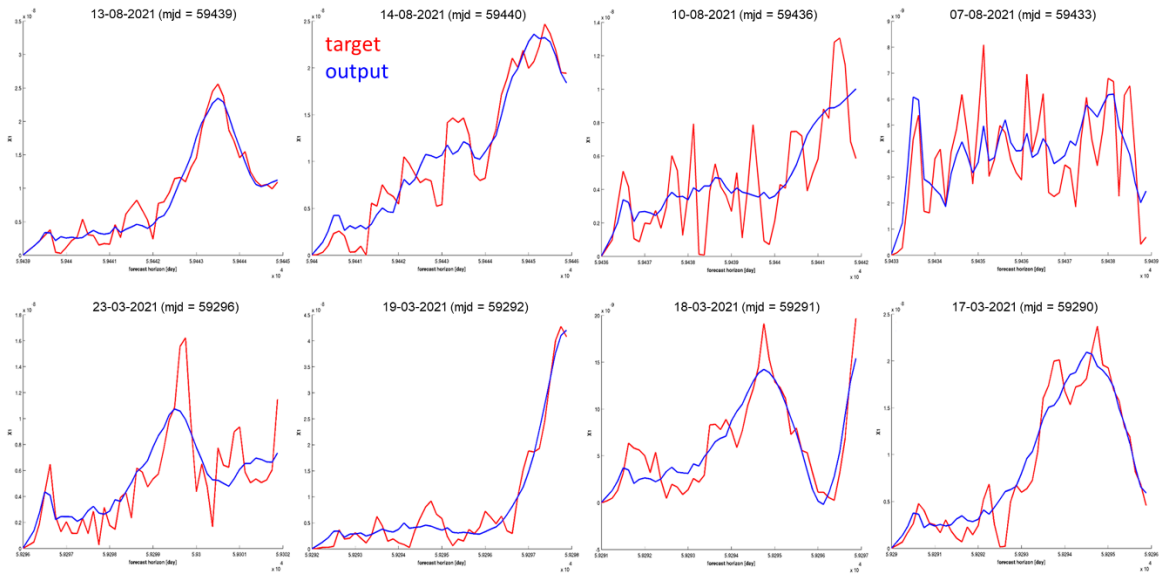


Figure 5. Neural network to predict the level of uncertainty of EAM forecast. Training and input data is the absolute value of the difference between EAM forecast and EAM analysis. The target and output is the level of uncertainty of the EAM forecast.

3. CONCLUSIONS

While analyzing EAM forecast errors contained in the ESMGFZ prediction products, we found predominantly normal error distributions in the OAM and HAM mass and motion terms. As expected, the error increases generally with prediction length. This error is introduced in the ocean and hydrological model forecast runs by the rapidly decreasing prediction skill after day 5 of the atmospheric forecast data, which is the most important input to both the ocean and the land surface model. Long-term processes excited in the ocean and hydrological model are able to enhance the model-derived EAM forecast prediction skill after 5 days into the future. However, we also found large systematic error contributions in the AAM X_1 and X_2 motion terms that dominate the very first forecast epochs. This error originates in the artificial wind signals that are excited in the ECMWF atmospheric weather forecast system after the end of the data assimilation window that constrains the ECMWF model. We were able to identify the patterns of such systematic error contributions with a machine learning approach. Such a systematic error can be predicted for every new forecast depending on the characteristics of a few past forecasts. Correcting for the systematic error, the prediction skill of AAM equatorial wind terms is significantly improved, leading finally to improved polar motion predictions during the first 10 forecast days. The remaining error follows a more or less stochastic error distribution. The stochastic error part cannot be predicted and removed, but we were able to estimate at least the level of uncertainty for the EAM forecasts, apart from sub-daily variations. One might overcome this drawback by using only daily values of EAM forecasts for daily

sampled EOP predictions. As soon as we implement the EAM forecast error estimation in the routinely processing environment, we will provide these uncertainty estimates along with our deterministic EAM forecast products for further use in EOP prediction methods like, for example, Kalman filters.

Acknowledgements. This study was carried out in the framework of the second Earth orientation parameter prediction comparison campaign (EOPPCC). All EAM analysis and forecast data sets used in this study are available from the ESMGFZ EAM data portal http://esmdata.gfz-potsdam.de:8080/repository. Analysis and machine learning models have been carried out with MATLAB.

REFERENCES

Barnes, R. T. H., Hide, R., White, A. A., Wilson, C. A. (1983) Atmospheric angular momentum fluctuations, length-of-day changes and polar motion. Proc. R. Soc. Lond., A Math. phys. sci., (1792), 31-73. https://doi.org/10.1098/rspa.1983.0050

Bell, M. J., Hide, R., Sakellarides, G. (1991) Atmospheric angular momentum forecasts as novel tests of global numerical weather prediction models. Philosophical Transactions of the Royal Society of London. Series A: Physical and Engineering Sciences, 334, 55–92. https://doi.org/10.1098/rsta.1991.0003.

Brzezinski, A. (1992) Polar motion excitation by variations of the effective angular momentum function: considerations concerning deconvolution problem. Manuscr. Geod., 17 , 3-20.

Dill, R., Dobslaw, H. (2010) Short-term polar motion forecasts from earth system modeling data. J. Geodesy, 84 (9), 529-536. https://doi.org/10.1007/s00190-010400 -0391-5.

Dill, R., Dobslaw, H., Thomas, M. (2013) Combination of modeled shortterm angular momentum function forecasts from atmosphere, ocean, and hydrology with 90-day EOP predictions. J. Geodesy, 87 (198), 567-577. https://doi.org/10.1007/s00190-013-0631-6.

Dill, R., Dobslaw, H., Thomas, M. (2018) Improved 90-day Earth orientation predictions from angular momentum of atmosphere, ocean, and terrestrial hydrosphere. J. Geodesy, 92. https://doi.org/10.1007/s00190-018-1158-7.

Dill, R., Dobslaw, H., Thomas, M. (2019) Improved 90-day Earth orientation predictions from angular momentum forecasts of atmosphere, ocean, and terrestrial hydrosphere. J. Geodesy, 93, 3, 287-295. https://doi.org/10.1007/s00190-018-1158-7.

Dill, R., Saynisch-Wagner, J, Irrgang, C., Thomas, M. (2021) Improving atmospheric angular momentum forecasts by machine learning. Earth and Space Science, 8. Earth and Space Science, 8. https://doi.org/10.1029/2021EA002070.

Dobslaw, H., & Dill, R. (2017) Predicting Earth Orientation Changes from Global Forecasts of Atmosphere-Hydrosphere Dynamics. Advances in Space Research. https://doi.org/10.1016/j.asr.2017.11.044.

Freedman, A. P., Steppe, J. A., Dickey, J. O., Eubanks, T. M., & Sung, L. Y. (1994) The short-term prediction of universal time and length-of-day using atmospheric angular momentum. Journal of Geophysical Research, 99(B4), 6981–6996. https://doi.org/10.1029/93JB02976.

Gou, J., Kiani Shahvandi, M., Hohensinn, R., & Soja, B. (2023). Ultra-short-term prediction of LOD using LSTM neural networks. J Geod 97, 52. https://doi.org/10.1007/s00190-023-01745-x

Kiani, MS., & Soja, B. (2022). Inclusion of data uncertainty in machine learning and its application in geodetic data science, with case studies for the prediction of Earth orientation parameters and GNSS station coordinate time series. Advances in Space Research, 70(3), 563-575. https://doi.org/10.1016/j.asr.2022.05.042

Kiani, MS., Gou, J., Schartner, M., & Soja, B. (2022a). Data Driven Approaches for the Prediction of Earth's Effective Angular Momentum Functions. In IGARSS 2022-2022 IEEE International Geoscience and Remote Sensing Symposium (pp. 6550-6553). IEEE. https://doi.org/10.1109/IGARSS46834.2022.9883545

Kiani, MS., Schartner, M., & Soja, B. (2022b). Neural ODE differential learning and its application in polar motion prediction. Journal of Geophysical Research: Solid Earth, 127(11), e2022JB024775. https://doi.org/10.1029/2022JB024775

Kur, T., Dobslaw, H., Śliwińska, J., Nastula, J., Wińska, M., & Partyka, A. (2022) Evaluation of selected short-term predictions of UT1-UTC and LOD collected in the second earth orientation parameters prediction comparison campaign. Earth, Planets and Space, 74(1), 1-9. https://doi.org/10.1186/s40623-022-01753-9

Modiri, S., Belda, S., Hoseini, M., Heinkelmann, R., Ferrándiz, J. M., & Schuh, H. (2020). A new hybrid method to improve the ultra-short-term prediction of LOD. Journal of geodesy, 94, 1-14. https://doi.org/10.1007/s00190-020-01354-y

Von Storch, H., Zwiers, F. W. (1999) Forecast quality evaluation. In Statistical analysis in climate research (p. 391-406). Cambridge University Press. https://doi.org/ 10.1017/CBO9780511612336.019.

Received: *2023-05-25*

Reviewed: *2023-08-29 (undisclosed name); 2023-09-25 (undisclosed name)*

Accepted: *2023-12-04*